EAS Journal of Nutrition and Food Sciences
Abbreviated Key Title: EAS J Nutr Food Sci
ISSN: 2663-1873 (Print) & ISSN: 2663-7308 (Online)
Published By East African Scholars Publisher, Kenya

OPEN ACCESS

Volume-8 | Issue-2 | May-Jun; 2026 | DOI: https://doi.org/10.36349/easjnfs.2026.v08i02.008

Original Research Article

Preparation and Properties of Ginger Essential Oil-Loaded Composite Nanoemulsions

Xinghai Yao[1]*, Huiqiong Ban[1], Zimei Jin[1]

[1]Gansu Polytechnic College of Animal Husbandry and Engineering, Wuwei 733006

Article History
Received: 02.05.2026
Accepted: 16.06.2026
Published: 18.06.2026

Journal homepage:
https://www.easpublisher.com

Quick Response Code

Abstract: To improve the stability and bioavailability of ginger essential oil (GEO), the optimal ultrasonic power, Tween 80 addition amount, and GEO addition amount for preparing ginger essential oil-Tween 80 nanoemulsions (GEO-T80NE) were first screened via single-factor experiments and orthogonal experiments using particle size and encapsulation efficiency as indicators. Based on these findings, carboxymethyl chitosan (CMCS) was utilized as a composite emulsifier in an equal ratio to Tween 80 to prepare ginger essential oil composite nanoemulsions (GEOCNs). The results indicated that under 15 min of ultrasonic treatment, the optimal process parameters for GEO-T80NE preparation were an ultrasonic power of 320 W, 3% Tween 80, and 4% GEO. The resulting GEO-T80NE exhibited an average particle size of 268.00 ± 1.53 nm and an encapsulation efficiency of 88.50 ± 0.17%. When an equal proportion of CMCS was added, the prepared GEON-CMCS demonstrated an average particle size of 284.67 ± 0.58 nm. Furthermore, at 46 °C, the average particle size of GEOCNs was 48% smaller than that of GEO-T80NE, demonstrating effectively enhanced temperature stability. Additionally, the scavenging rates of GEOCNs against DPPH and ABTS free radicals increased by 17.47% and 9.94%, respectively. In conclusion, the combined application of CMCS and Tween 80 effectively improves the physical stability and functional properties of GEO-T80NE, offering a valuable reference for its application in the food, pharmaceutical, and other related industries.

Keyword: Ginger Essential Oil, Nanoemulsion, Preparation Process, Stability, Antioxidant Activity.

1 INTRODUCTION

Ginger essential oil (GEO) is rich in active components such as zingiberene, gingerol, and citral, exhibiting broad-spectrum antibacterial and antioxidant properties that reveal immense application potential in the food sector [1]. However, its poor stability, high volatility, and low aqueous solubility significantly restrict the exertion of its functionalities [2]. Nanoemulsions, characterized by a small droplet size, large specific surface area, and excellent substance solubility, serve as carrier systems capable of encapsulating hydrophobic essential oils within nanoscale droplets. This encapsulation effectively improves the dispersibility, stability, and bioavailability of the essential oils [3].

As a commonly utilized non-ionic surfactant, Tween 80 effectively reduces oil-water interfacial tension, making it an ideal emulsifier for constructing essential oil nanoemulsions. Lan Weiqing *et al*., [4], demonstrated that emulsions prepared using Tween 80 as an emulsifier exhibited strong inhibitory effects against *Shewanella putrefaciens*. Nonetheless, traditional single-surfactant systems often present limitations regarding emulsion stability, particularly when encountering complex oil-water interfaces, where phase separation frequently occurs. Furthermore, single-emulsifier systems provide limited synergistic enhancement to the functional activities (e.g., antibacterial and antioxidant capabilities) of essential oils. Carboxymethyl chitosan (CMCS) is a highly water-soluble chitosan derivative that not only possesses excellent film-forming, antibacterial, and antioxidant properties but also significantly bolsters emulsion stability via steric hindrance and electrostatic repulsion [5].

Based on these considerations, this study first optimized critical parameters—including ultrasonic power and the addition amounts of GEO and Tween 80—through single-factor experiments and orthogonal

***Corresponding Author:** Xinghai Yao
Gansu Polytechnic College of Animal Husbandry and Engineering, Wuwei 733006

experiments. The objective was to acquire a ginger essential oil-Tween 80 nanoemulsion (GEO-T80NE) featuring the smallest particle size and the most uniform distribution. Subsequently, building upon the optimal GEO-T80NE preparation process, CMCS (at a concentration equal to Tween 80) was incorporated as a natural polysaccharide stabilizer to fabricate ginger essential oil composite nanoemulsions (GEOCNs). The stability, antioxidant capacity, and antibacterial properties of the resulting emulsions were evaluated. The findings of this research aim to facilitate the development of nanoemulsions with superior functional activity and stability, thereby providing technical guidance for the highly efficient utilization of ginger essential oil.

2 MATERIALS AND METHODS

2.1 Materials

Ginger essential oil was acquired from Tongmei Food Technology Co., Ltd. Tween 80 (chemically pure) was sourced from Tianjin Meilin Industry and Trade Co., Ltd. Carboxymethyl chitosan (degree of substitution > 80%) was supplied by Adamas Reagent Co. DPPH and ABTS were purchased from Shandong Keyuan Biochemical Co., Ltd. Absolute ethanol (analytical grade) was procured from Sinopharm Chemical Reagent Co., Ltd.

2.2 Experimental Methods

2.2.1 Preparation of Ginger Essential Oil Nanoemulsion (GEONE)

The methodology described by Liu Mengmeng *et al*., [6], was adopted with slight modifications. The aqueous phase was slowly dripped into the GEO and homogenized using a high-pressure homogenizer for 2 min to ensure thorough mixing, producing a coarse emulsion. This coarse emulsion was then subjected to ultrasonic circulation treatment for 15 min to yield the final ginger essential oil nanoemulsion.

2.2.2 Preparation Process Optimization of Ginger Essential Oil-Tween 80 Nanoemulsion (GEO-T80NE)

Using the average particle size and encapsulation efficiency of the emulsion as evaluation metrics, three independent variables were adjusted to define their optimal ranges: GEO addition (4%, 6%, 8%, 10%, 12%), Tween 80 addition (1%, 2%, 3%, 4%, 5%), and ultrasonic power (160 W, 240 W, 320 W, 400 W, 480 W). Following the single-factor experiments, a 3-factor, 3-level orthogonal experimental design was implemented. The optimal preparation parameter combination was determined primarily based on the average particle size of the nanoemulsions.

2.2.3 Preparation of Composite Nanoemulsions (GEOCNs)

The preparation of the CMCS emulsion was adapted from the protocol outlined by Jia Liao [7]. Specifically, 1 g of carboxymethyl chitosan was added to 99 mL of deionized water and slowly mixed via magnetic stirring until evenly dispersed. The mixture was stored overnight at 4 °C to allow for complete hydration.

For the preparation of GEOCNs, parameters such as ultrasonic power, sonication time, and the amounts of Tween 80 and GEO adhered to the optimal conditions identified in section 2.2.2. The samples were divided into four groups: Group A, GEO-T80NE prepared exclusively with Tween 80 in the aqueous phase; Group B, GEO-CMCS prepared utilizing an equal proportion of CMCS in the aqueous phase; Group C, GEOCNs prepared by blending CMCS and Tween 80 in equal proportions; and Group D, consisting of pure essential oil. All samples were homogenized for 2 min, followed by 15 min of ultrasonic emulsification, ultimately yielding the respective nanoemulsions.

2.2.4 Particle Size Determination

Following a modified version of the method by Lan Weiqing *et al*., [4], a laser nanometer particle size analyzer was utilized to measure the emulsion droplet size. Prior to analysis, the emulsion was diluted 100-fold with deionized water. The diluted sample was added dropwise into a sample cell pre-filled with deionized water, and measurements commenced once the obscuration level reached 8% to 20%. The refractive index of the GEO sample was set to 1.491, its absorption rate to 0.001, and the medium refractive index to 1.33. Each sample was analyzed in triplicate.

2.2.5 Encapsulation Efficiency Determination

Measurements were conducted referencing the modified method of Tu Qian [8]. Initially, the maximum absorption peak of GEO was established. Subsequently, 0.5 mL of the emulsion was mixed with 4.5 mL of absolute ethanol in a 50 mL centrifuge tube and centrifuged at 8000 r/min for 10 min. The supernatant was diluted 1000 times, and its absorbance was measured at the maximum absorption peak utilizing a UV-Vis spectrophotometer. The concentration of the free oil phase was interpolated from a standard curve, and the encapsulation efficiency (EE, %) was calculated using Equation (1):

$$EE(\%)=\frac{C_0 - C}{C_0}\times 100\% \quad (1)$$

Where *EE* represents the encapsulation efficiency (%), C_0 is the total volume of essential oil initially added (mL), and *C* denotes the volume of free essential oil (mL).

2.2.6 Stability Determination

Temperature stability evaluations were based on the modified method of Zhang Keke [9]. The nanoemulsions were stored at different temperatures (-4 °C, 25 °C, 46 °C) for 24 h, after which their stability was assessed by measuring particle size. Storage stability was assessed referencing the modified method of Bai Shiru [10]. Freshly prepared nanoemulsions were transferred into transparent glass vials and stored at -4 °C. The

macroscopic appearance of the emulsions was recorded photographically at 0, 7, 14, and 21 days. Concurrently, microstructural alterations in the emulsions were monitored using optical microscopy.

2.2.7 Antioxidant Activity Analysis

The DPPH free radical scavenging assay was performed according to the method of Gharibzahedi [11], with slight modifications. A precise amount of DPPH was dissolved in absolute ethanol to prepare a 0.08 mg/mL DPPH solution. A 2 mL aliquot of the emulsion was mixed with 2 mL of the DPPH solution. Following thorough mixing, the solution was incubated at room temperature for 30 min, and the absorbance of the upper solution was read at 517 nm. The ABTS free radical scavenging assay was adapted from Shao Xinman *et al*., [12]. An ABTS radical stock solution was generated by mixing equal volumes of 7 mM ABTS solution and 5 mM potassium persulfate solution. The mixture was left to react in the dark for 12 h to stabilize. This stock solution was then suitably diluted with absolute ethanol until its absorbance at 734 nm reached 0.70 ± 0.02. For the assay, 20 µL of the sample was combined with 2 mL of the diluted ABTS working solution and allowed to react in the dark for 30 min. The final absorbance of the mixture was recorded at 734 nm using a UV-Vis spectrophotometer.

2.2.8 Antibacterial Study

Referring to the method of Sun *et al*., [13], Gram-negative bacteria (*Escherichia coli*) and Gram-positive bacteria (*Staphylococcus aureus*) were utilized as the test microorganisms. A volume of 100 µL of bacterial suspension (1×10^7 CFU/mL) was evenly distributed onto LB agar plates using a sterile spreader. Sterile Oxford cups were positioned on the agar surface, and 100 µL of the respective emulsion was pipetted into each cup; sterile water served as the blank control. The plates were incubated in a thermostatic chamber at 37 °C for 24 h, after which the inhibition zone diameters were measured utilizing the cross-measurement method.

2.3 Data Processing and Statistical Analysis

All experiments were performed in triplicate, and data are presented as the mean ± standard deviation. Analysis of variance (ANOVA) followed by Duncan's multiple range test was conducted using SPSS 22.0, with a significance threshold set at $P < 0.05$. Graphical representations were constructed using GraphPad Prism 10.

3 RESULTS AND DISCUSSION

3.1 Single-Factor Experiment Result Analysis

3.1.1 Effect of GEO Addition on the Particle Size and Encapsulation Efficiency of GEO-T80NE

As depicted in Figure 1a, the average particle size of the emulsion exhibited a significant ascending trend with the incremental addition of GEO ($P \leq 0.05$). The emulsion achieved its minimum average particle size (259 nm) at a GEO mass fraction of 4%. Conversely, when the GEO mass fraction escalated to 12%, the average particle size notably expanded to 404 nm. This implies that at lower oil phase concentrations, the available emulsifier adequately covers the interfacial area, thus facilitating the formation of fine, stable droplets. However, continuous augmentation of GEO results in a relative emulsifier deficit, rendering it incapable of preventing inter-droplet collisions and fusion. This ultimately precipitates emulsion aggregation or Ostwald ripening, driving the increase in particle size [14]. Figure 1b reveals that the encapsulation efficiency of the emulsion steadily declined in tandem with increased GEO loading. Maximum encapsulation efficiency (91.50 ± 0.20%) occurred at 4% GEO. As the essential oil input reached 10%, the encapsulation rate experienced a significant drop ($P \leq 0.05$). These findings indicate a specific loading threshold of the emulsifier for GEO; surpassing this threshold causes a portion of the GEO to remain unencapsulated, leading to reduced encapsulation efficiency. Balancing the dynamics of both particle size and encapsulation efficiency, GEO addition levels of 4%, 6%, and 8% were advanced for the subsequent orthogonal optimization trials.

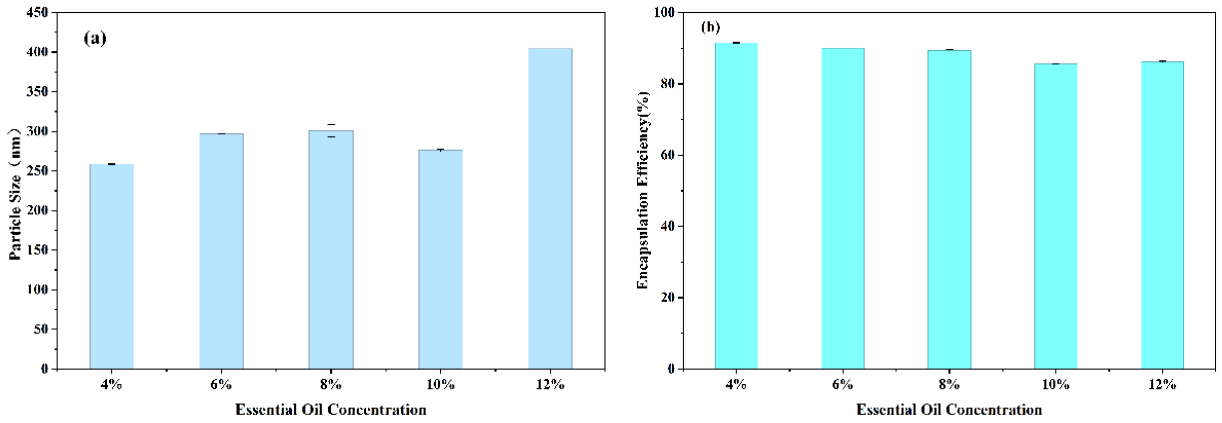

Figure 1: Effects of different essential oil additions on emulsion particle size (a) and encapsulation efficiency (b)

3.1.2 Effect of Tween 80 Addition on the Particle Size and Encapsulation Efficiency of GEO-T80NE

Figure 2a demonstrates that elevating the Tween 80 concentration generally induced a reduction in emulsion particle size. A Tween 80 concentration of 4% yielded the smallest average particle size (203 nm). This aligns with findings from Yang Tiyuan *et al*., [15], who posited that an enhanced adsorption rate at the oil-water interface gradually diminishes interfacial tension, subsequently reducing droplet size. According to Figure 2b, escalating Tween 80 usage initially prompted a rise in encapsulation efficiency, peaking at 78.50 ± 0.01% with 3% Tween 80, before experiencing a subsequent decline. This suggests that while an optimal quantity of Tween successfully envelops the active compounds, exceeding the system's critical micelle concentration deteriorates the encapsulation efficacy. This outcome parallels the experimental results documented by Wang Lin [16]. Consequently, Tween 80 concentrations of 2%, 3%, and 4% were selected for further orthogonal optimization.

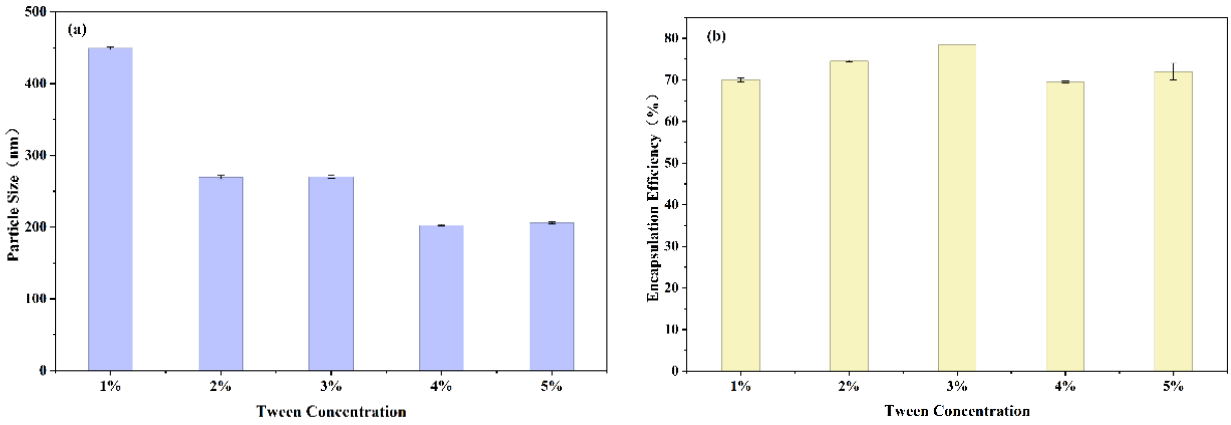

Figure 2: Effects of different Tween 80 concentrations on emulsion particle size (a) and encapsulation efficiency (b)

3.1.3 Effect of Ultrasonic Power on the Particle Size and Encapsulation Efficiency of GEO-T80NE

As illustrated in Figure 3a, ultrasonic dispersion achieved optimal efficacy at 320 W, generating emulsions with the smallest average particle size (274.00 nm). This demonstrates that the intense shear forces produced at this specific power level are capable of disrupting the emulsion and facilitating effective dispersion by the emulsifier particles [11]. Nevertheless, further elevation in ultrasonic power resulted in larger particle sizes, an observation consistent with the conclusions reported by Chai Yuxing *et al*., [17]. Figure 3b indicates that the maximum encapsulation efficiency of GEO-T80NE (72.00 ± 1.59%) was obtained at 240 W; power levels exceeding 240 W triggered a marked decline in encapsulation efficiency ($P < 0.05$). Considering all factors, ultrasonic powers of 160 W, 240 W, and 300 W were chosen for the subsequent orthogonal testing.

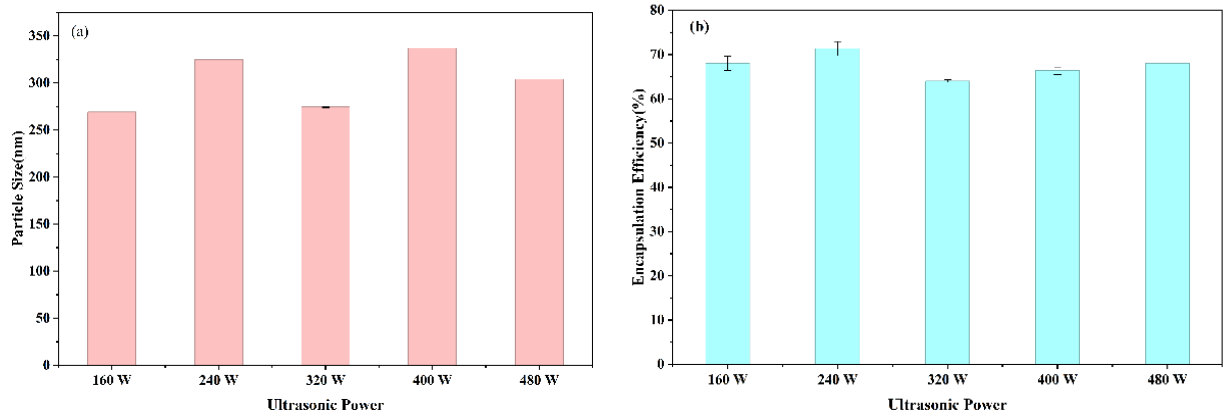

Figure 3: Effects of different ultrasonic powers on emulsion particle size (a) and encapsulation efficiency (b)

3.2 Analysis of Orthogonal Test Results

Building upon the single-factor experiments, a 3-factor, 3-level orthogonal experimental array was constructed using particle size as the primary criterion to optimize GEO addition (A), Tween 80 addition (B), and ultrasonic power (C). The design matrix is detailed in

Table 1, and the resulting experimental data are summarized in Table 2.

Table 1: Orthogonal experimental design

Factor Level	GEO Concentration (%)	Tween 80 Concentration (%)	Ultrasonic Power (W)
1	4	2	160
2	6	3	240
3	8	4	320

Table 2: Results of orthogonal experiment

Sample	Factors			Particle Size (nm)
	GEO Concentration (A)	Tween 80 Concentration (B)	Ultrasonic Power (C)	
1	1	1	1	279.00±5.29
2	1	2	3	268.00±1.53
3	1	3	2	299.00±5.51
4	2	1	3	279.00±2.08
5	2	2	2	282.00±0.58
6	2	3	1	281.00±0
7	3	1	2	305.00±0.58
8	3	2	1	317.00±0.58
9	3	3	3	289.00±0
K1	282	288	283	
K3	304	290	279	
R	23	2	4	
Order of factor influence				
Optimal combination		$A_1B_2C_3$		

As shown in Table 2, the Range (R) values reveal that the hierarchy of influence of the three factors on the emulsion parameters is B > C > A. This indicates that the addition amount of Tween exerts the most significant influence on the emulsion, followed by ultrasonic power. Assuming a constant ultrasonic duration of 15 min, the optimal parameter combination derived from the orthogonal test was A1B2C3, corresponding to 4% essential oil addition, 3% Tween addition, and 320 W ultrasonic power. The emulsion synthesized under these optimal conditions possessed a particle size of 268.00 ± 1.53 nm alongside an encapsulation efficiency of 88.50 ± 0.17%.

3.3 Stability Analysis of GEOCNs

3.3.1 Temperature Stability Analysis

As observed in Figure 4, freshly prepared GEOCNs and GEO-T80NE displayed no significant difference in particle size. This confirms that both emulsifier configurations effectively encapsulate the essential oil, imparting robust initial stability to the emulsions, and that the introduction of CMCS imposes minimal impact on the inherent particle size of GEO-T80NE. Nonetheless, under varying temperature storage regimes, the particle sizes across the four emulsion groups diverged significantly. Notably, the stability of the GEO-CMCS group proved substantially inferior to the other three groups, a phenomenon likely linked to the regulatory capacity of the specific CMCS concentration on the emulsion's particle size. Closer inspection showed that during storage at -4 °C and 25 °C, the particle sizes of GEOCNs and GEO-T80NE remained statistically comparable. However, exposure to 46 °C induced a significant discrepancy: the average particle size of GEOCNs was 48% smaller than that of GEO-T80NE. This evidence underscores the superior capability of the composite emulsifier system to preserve emulsion stability under elevated temperatures. Optical micrographs corroborate this, showing that droplets in groups A and C were consistently fine and structurally stable across the tested temperature range. In contrast, droplets in group B swelled at different temperatures, exhibiting mild aggregation, while group D suffered from severe droplet aggregation, pronounced structural heterogeneity, and eventual demulsification—matching the particle size data. Conclusively, supplementing the optimally formulated GEO-T80NE with CMCS dramatically improves its thermal stability.

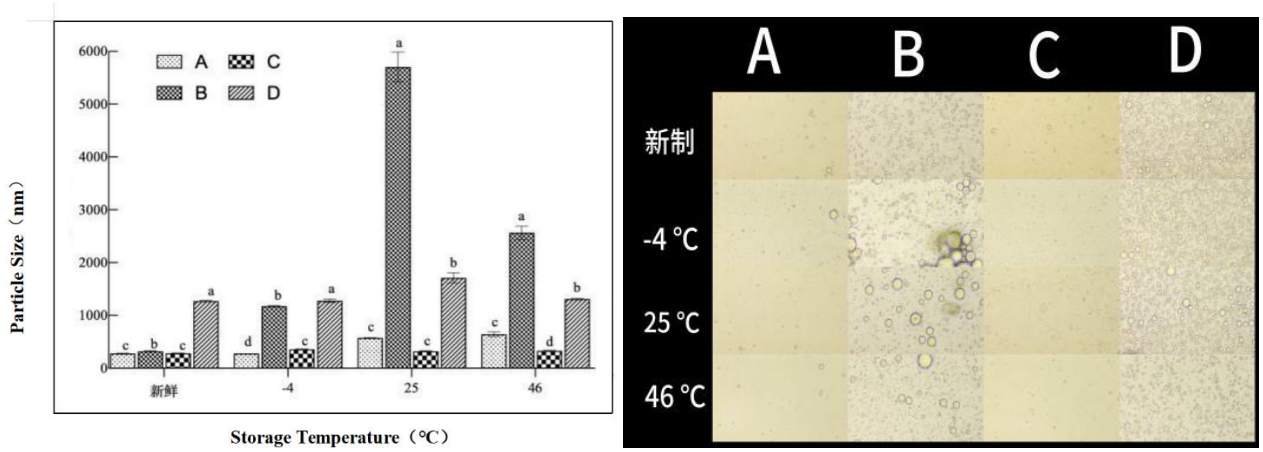

Figure 4: Changes in particle size and morphology under optical microscope of emulsions at different temperatures

3.3.2 Storage Stability Analysis

As presented in Figure 5, the freshly prepared emulsion samples were highly uniform, devoid of any discernible stratification. Following 7 days of storage, mild stratification or phase separation emerged in groups B and D. Extending the storage period to 14–21 days exacerbated this instability in groups B and D, leading to localized transparent or translucent separation layers. This indicates a significant decrease in the stability of these groups over prolonged storage. Conversely, groups A and C exhibited no stratification throughout the duration, though group C exhibited comparatively higher viscosity. This heightened viscosity stems from the augmented viscoelasticity of the emulsion imparted by CMCS, which successfully curtails the frequency of inter-droplet collisions [18]. Optical microscopy validated these macroscopic observations: at day 7, groups A and C maintained homogeneous, fine droplet dispersions, whereas groups B and D presented large agglomerated particles and entrapped air bubbles. This indicates an impaired emulsifier adsorption capacity or disrupted inter-droplet interactions in the latter groups. By day 14, particle abundance and heterogeneous distribution had amplified in groups B and D, progressing to extensive droplet clustering and structural destabilization by day 21. These findings suggest that using 3% CMCS independently as the aqueous phase fails to achieve optimal emulsification, potentially due to an unoptimized concentration. Conversely, synthesizing an emulsion with an equimolar ratio of CMCS and Tween 80 remarkably elevated systemic stability. Future studies should prioritize fine-tuning the exact addition ratio of CMCS. Collectively, macroscopic appearance and microstructural imagery confirm that groups A and C retain excellent stability even after 21 days of storage at -4 °C.

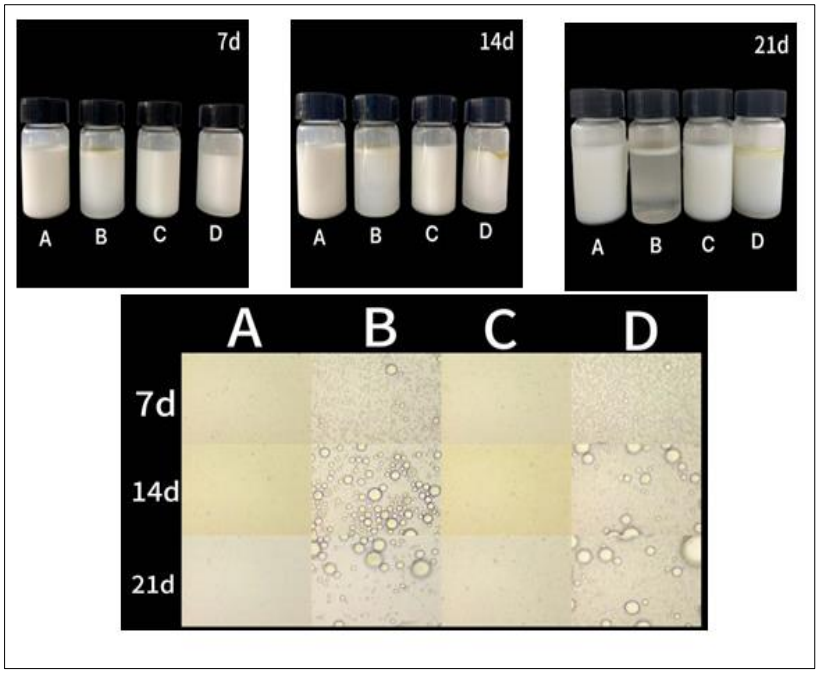

Figure 5: Changes of emulsions during storage at -4 °C

3.4 Antioxidant Analysis of GEOCNs

The DPPH and ABTS free radical scavenging assays were utilized to determine the antioxidant activity of the free GEOCNs, with outcomes plotted in Figure 6. All experimental groups displayed significantly distinct antioxidant activities ($P < 0.05$). Although group C's DPPH scavenging ability was significantly lower than that of the pure essential oil group, it still achieved a robust scavenging rate of approximately 63.32%. This performance was 17.47% and 34% superior to groups A and B, respectively. Regarding the ABTS free radical scavenging assay, group C recorded a scavenging rate of 82.430 ± 0.002%, displaying no statistically significant divergence from the pure essential oil control group ($P < 0.05$). This proves that formulating GEO into GEOCNs does not compromise the intrinsic antioxidant attributes of the essential oil. Overall, the free radical scavenging rate of GEOCNs considerably surpassed that of GEO-T80NE. This enhanced functionality is largely attributable to CMCS; beyond serving as an emulsifier, the CMCS molecular structure hosts active functional moieties (e.g., amino, hydroxyl, and carboxymethyl groups) capable of donating hydrogen atoms, thereby interacting with and neutralizing free radicals [3]. Moreover, when Tween 80 and CMCS function concurrently within the aqueous phase, the highly stable interfacial barrier formed by Tween promotes a more homogeneous distribution of CMCS across the oil-water interface and throughout the emulsion matrix. This optimal spatial arrangement allows the antioxidant active sites on CMCS to comprehensively engage and capture free radicals, synergistically boosting the total antioxidant capacity of GEOCNs [19].

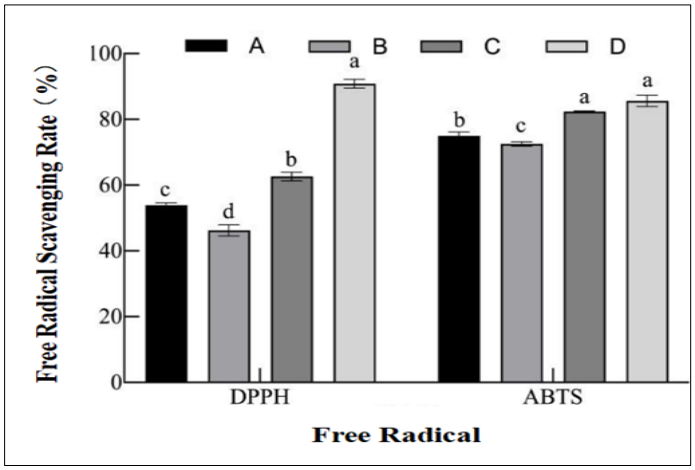

Figure 6: Scavenging ability of emulsions against DPPH free radicals and ABTS free radicals

4 CONCLUSION

In this study, using emulsion average particle size and encapsulation efficiency as primary benchmarks, single-factor orthogonal experiments were executed to optimize the formulation parameters for GEO-T80NE employing Tween 80 as the primary emulsifier. Assuming a fixed 15 min ultrasonic treatment, the optimum processing conditions were established as: 320 W ultrasonic power, 3% Tween 80 addition, and 4% GEO addition. Under this optimized protocol, the resultant GEO-T80NE possessed an average particle size of 268.00 nm and an encapsulation efficiency of 88.50 ± 0.17%. Expanding upon these parameters, CMCS was introduced in an equal mass proportion to act as a composite emulsifier, a strategy engineered to drastically bolster both physical stability and the sustained release of active compounds. The findings confirmed that freshly synthesized GEOCNs featured an average particle size of 284.67 nm, showing no significant difference compared to GEO-T80NE. In terms of storage stability, at temperatures of -4 °C and 25 °C, the average particle sizes of GEOCNs and GEO-T80NE were functionally identical. However, under thermal stress at 46 °C, the average particle size of GEOCNs was 48% smaller than its GEO-T80NE counterpart, verifying a vastly improved thermal stability profile. Additionally, the composite nanoemulsion preserved its stability after 21 days of continuous storage at -4 °C. Functionally, GEOCNs exhibited a 17.47% and 9.94% augmentation in DPPH and ABTS free radical scavenging rates, respectively, when compared to GEO-T80NE, highlighting a substantial leap in antioxidant potency. In summary, combining CMCS and Tween 80 not only rectifies the physical vulnerabilities of single-emulsifier GEONEs but also significantly amplifies their antioxidant and antibacterial properties, presenting a potent novel technological framework for application in the food, biomedical, and adjacent industries.

Acknowledgments

Fund Project: 2025 Gansu Provincial University Teachers' Innovation Fund Project

Project No.: 2025A-381

REFERENCES

1. GUO J G, YANG S, WU Y H, et al. Preparation of ginger essential oil microcapsules and its effect on the quality of chilled pork [J]. Journal of Chinese Institute of Food Science and Technology, 2025, (2): 342-352.

2. LONG Y, HUANG W, WANG Q, et al. Green synthesis of garlic oil nanoemulsion using ultrasonication technique and its mechanism of antifungal action against Penicillium italicum [J]. Ultrason Sonochem, 2020, 64: 104970.
3. ZHANG X, WANG Y, WANG D, et al. Synergistic stabilization of garlic essential oil nanoemulsions by carboxymethyl chitosan/Tween 80 and application for coating preservation of chilled fresh pork [J]. Int J Biol Macromol, 2024, 266: 131370.
4. LAN W Q, ZHAO J X, XIE J. Preparation of carvacrol nanoemulsion and its inhibitory effect on Shewanella putrefaciens [J]. Journal of Guangdong Ocean University (Natural Science Edition), 2024, 0(3): 8.
5. XU Y, WANG S, XIN L, et al. Interfacial mechanisms, environmental influences, and applications of polysaccharide-based emulsions: A review [J]. Int J Biol Macromol, 2025, 293: 139420.
6. LIU M M, GUO S Y, XIAO H, et al. Optimization of preparation process and stability of zingerone nanoemulsion [J]. Journal of Chinese Institute of Food Science and Technology, 2024, 24(2): 120-129.
7. JIA L A, WANG Y Y, KOU K, et al. Effect of pH-shift pretreatment on walnut protein-carboxymethyl chitosan composite particles and their application in high internal phase Pickering emulsions [J]. Food and Fermentation Industries: 1-15[2025-09-28].
8. TU Q. Preparation of sodium alginate-chitosan modified cinnamon essential oil liposomes and their application in chilled pork [D]. Sichuan Agricultural University.
9. ZHANG K K, ZOU H J, FAN Y, et al. Preparation of highly stable O/W Pickering emulsions based on amphiphilic Janus-SiO2 particles [J]. China Surfactant Detergent & Cosmetics (Chinese and English), 2025, 55(3): 271-278.
10. BAI S R, TANG L, FAN B, et al. Optimization of preparation process and stability of peppermint essential oil nanoemulsion [J]. Food Science and Technology, 2025, 50(1): 265-274.
11. GHARIBZAHEDI S M T, ALTINTAS Z. Eryngo essential oil nanoemulsion stabilized by sonicated-insect protein isolate: An innovative edible coating for strawberry quality and shelf-life extension [J]. Food Chem, 2025, 463: 141150.
12. SHAO X M, CHENG C, DENG Q C, et al. Effect of natural pomelo peel essential oil on the physicochemical stability of flaxseed oil and its emulsion system [J]. China Oils and Fats: 1-13[2025-09-28].
13. SUN Y, XU H, XIE Y, et al. Sulfonated cellulose nanocrystalline- and pea protein isolate-mixture stabilizes the citral nanoemulsion to maintain its functional activity for effectively preserving fruits [J]. Int J Biol Macromol, 2025, 289: 138725.
14. NIKITA, AGNIHOTRI S. Nanoemulsions as advanced delivery systems of bioactive compounds for sustainable food preservation applications [J]. Biocatal and Agr Biotech, 2025, 68: 103702.
15. YANG T Y, FANG Z Z, ZHAO L Y, et al. Preparation process and properties of allicin nanoemulsion [J]. Food Science and Technology, 2024, 49(4): 269-277.
16. WANG L, DU W C, YA Q, et al. Preparation process and stability of astaxanthin emulsion [J]. The Food Industry, 2024, 45(12): 61-65.
17. CHAI Y X, XU Y Y, HUANG S T, et al. Process optimization and antioxidant activity of whey protein isolate-inulin based ginsenoside nanoemulsion prepared by ultrasound-assisted high pressure microfluidization [J]. Food Research and Development, 2025, (7): 76-84.
18. LI L, GENG M, TAN X, et al. Insight on the interaction between soybean protein isolate and ionic/non-ionic polysaccharides: Structural analysis, oil-water interface properties investigation and double emulsion formation [J]. Food Hydrocolloids, 2024, 150: 109754.
19. CHAUDHARY S. Chitosan nanoemulsion: A sustainable approach for quality preservation of fish and fishery foods [J]. Food Control, 2023, 151: 109790.

Cite This Article: Xinghai Yao, Huiqiong Ban, Zimei Jin (2026). Preparation and Properties of Ginger Essential Oil-Loaded Composite Nanoemulsions. *EAS J Nutr Food Sci, 8*(2), 89-96.